PCCP

PERSPECTIVE

View Article Online
View Journal | View Issue

Cite this: *Phys. Chem. Chem. Phys.*, 2014, **16**, 8721

Photoionization of clusters in intense few-cycle near infrared femtosecond pulses

S. R. Krishnan,*[a] R. Gopal,[a] R. Rajeev,[b] J. Jha,[b] V. Sharma,[c] M. Mudrich,[d] R. Moshammer[e] and M. Krishnamurthy*[ab]

Received 20th December 2013,
Accepted 18th March 2014

DOI: 10.1039/c3cp55380a

www.rsc.org/pccp

In this article we present a perspective on the current state of the art in the photoionization of atomic clusters in few-cycle near-infrared laser pulses. Recently, several studies have reported intriguing phenomena associated with the photoionization of clusters by pulses as short as ~10 fs which approach the natural timescales of collective electronic motion in such nanoscale aggregates. In contrast to the dynamics occurring on few- and sub-picosecond timescales where ionic motion sets in and plays a key role marked by resonant plasmon oscillations, the few-cycle limit precludes cluster expansion due to the nuclear motion of ionic constituents. Thus, pulses lasting just a few optical cycles explore a new "impulsive" regime for the first time in cluster nanoplasmas wherein ions essentially remain "frozen". Along with the perspective on this new regime, we present first measurements of photoelectron distributions and temperatures.

Introduction

The investigation of the photoionization of clusters in near-infrared (NIR) fields in the femtosecond domain has been a consequence of breakthroughs and developments in femtosecond laser technology. More recently, the availability of sufficiently intense few-cycle pulses[1] from Ti:Sapphire mode-locked systems has provided opportunities to study photoionization in isolated atoms[2] and molecules,[3–5] and in clusters. While the photoionization of rare-gas and metal clusters in long femtosecond pulses (pulse widths greater than 50 fs) has been studied for over two-decades now and adequately reviewed,[6,7] similar investigations with few-cycle pulses are rapidly gaining attention with contemporary and future efforts poised for exciting discoveries. Hence, a perspective on the current state of the art and an outlook towards forthcoming possibilities is timely.

These few-cycle near-infrared pulses, predominantly with a central wavelength of ~800 nm (photon energy ~1.5 eV), are said to be "intense" when the peak electric field is comparable to the Coulomb field binding the electron in an atom.[8] Under the influence of such an external electric field, bound electrons can tunnel out through the net potential which is a sum of the native atomic potential and that due to the laser pulse. The laser field acts as a strong time-varying external field which is highly perturbative[8,9] and cannot be understood within low-order perturbation theory. At a central wavelength of 800 nm, an optical cycle has a period of ~2.7 fs. Thus, pulses with a temporal full-width at half-maximum (FWHM) of 10 fs or less may be appropriately described as few-cycle pulses. Such pulses are so short that ionic motion during the interaction of these pulses with the target can be ruled out. Hence, these pulses provide an unprecedented opportunity to investigate clusters in a regime which is entirely dominated by electronic motion in the collective potential of the ions which remain motionless or "frozen" during the interaction with the pulse. In contrast, the photoionization dynamics of clusters in the NIR on sub- and few-picosecond timescales is dominated by the motion of ions – the expansion of the ionized aggregate leads to a strong resonant interaction between the driving laser field and the electron–ion system resulting in the so-called nanoplasma resonance. Fig. 1 provides a schematic illustration of an ensemble of clusters interacting with a focused beam of intense femtosecond pulses.

[a] *Tata Institute of Fundamental Research (Hyderabad), Hyderabad 50075, India. E-mail: srk@tifrh.res.in; Tel: +91 9440 264 291*
[b] *Tata Institute of Fundamental Research, 1 Homi Bhabha road, Mumbai 400001, India. E-mail: mkrism@tifr.res.in; Tel: +91 22 2278 2685*
[c] *Indian Institute of Technology – Hyderabad, Yeddumailaram, Hyderabad 502205, India*
[d] *Physikalisches Institut, Universität Freiburg, Hermann-Herder-Str. 3, 79104 Freiburg, Germany*
[e] *Max-Planck-Institut für Kernphysik, Saupferchekweg 1, D-69117 Heidelberg, Germany*

Generation of clusters – pure and doped

Atomic clusters used in photoionization studies are produced by the supersonic expansion of atoms in a gaseous state held at a pre-determined pressure and temperature before expansion through a tiny orifice. The dimensions of the orifice and the shape of the outlet together with the thermodynamic parameters

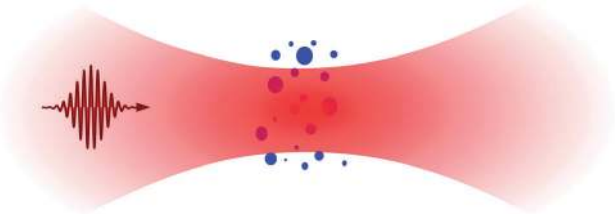

Fig. 1 Generic schematic of clusters (blue/black spheres) at the focus of a Gaussian beam of intense few-cycle near-infrared pulses, depicting the scenario discussed in the text. The sizes of clusters in this illustrative depiction are not to any scale.

determine the size of the atomic clusters which is a log-normal distribution.[10,11] This is captured using the Hagena parameter:[10,11]

$$\Gamma = k\, P_0 \cdot (d/\tan \alpha_{1/2})^{0.85} \cdot T_0^{-2.29}; \quad (1)$$

where P_0 is the pressure of the gas held at a temperature T_0 before expansion through the nozzle with an orifice diameter d and half-angle of opening $\alpha_{1/2}$. The parameter k depends on the gas being used and determines the propensity of cluster formation (see *e.g.* ref. 11, k = 3.85, 1650 and 5500 for He, Ar and Xe respectively). The number of atoms per cluster n is nearly quadratic in Γ with $n \sim \Gamma^q$; the value of q is in the range 1.8–2.25 depending on the gas.[10–12] While this scaling law is commonly used in the case of several rare-gas species, the sizes of helium clusters are often determined by comparing the conditions in use to the calibration curves found in extensive studies performed in the past, summarized by Stienkemeier *et al.*[13] and Toennies *et al.*[14] These jets have been produced in both the continuous[10] as well as pulsed[17] modes of operation.

Doping foreign species into host cluster matrices is done either by passing the jet of these pristine aggregates through a vapour cell containing the dopant atoms or by co-expanding a host–dopant gas mixture. One may also cross a jet of dopant atoms with the beam of host clusters to achieve the same result. For fine control of doping levels, the pick-up method is well-suited. In this case, the pick-up of dopants – rare-gases, metals or molecules – from the cell follows Poisson statistics as verified by several experiments[14,18] and Monte Carlo simulations.[19] These distributions should be taken into account in interpreting experimental results.

Photoionization of clusters in near-infrared fields – the long-pulse case

Nanoplasma resonance

It is appropriate to recapitulate the key aspects of the photoionization dynamics of rare-gas clusters in the long-pulse limit. Studies in this regime have been carried out with pulses 0.1–10 ps in duration or equivalently by twin-pulses separated by a variable delay on similar timescales. The most interesting properties of clusters in this domain result from the excellent absorption and coupling of energy from the laser field to the electron–ion system, the nanoplasma, far exceeding what is possible in atomic jets or planar solid targets.[6,7] This is due to the fact that the dipolar eigenfrequency (Ω) of collective electron oscillations, *i.e.* plasmons, in the quasi-neutral nanoplasma depends on the charge density ρ and the morphology of the nanoplasma, which for the spherical case is given by:[6,7]

$$\Omega^2 = 4\pi\rho/3; \quad (2)$$

In typical atomic clusters (1–100 nm in diameter), owing to the near-solid density of atoms, the nanoplasma eigenfrequency exceeds the central frequency of the IR pulses at 800 nm when the photoionization process begins.[6] This interaction can turn resonant due to ionic motion which sets in on timescales of ~0.1–1 ps when the cluster expands lowering the charge density. The decreasing nanoplasma eigenfrequency then matches the frequency of the driving laser field leading to the nanoplasma resonance.[6,15] This picture of dynamics, also called the nanoplasma model, has been validated by several experiments and *ab initio* numerical simulations on rare-gas and metal clusters (see *e.g.* ref. 6 and 7). Both charging of the cluster and absorption of light are enhanced if laser pulse-widths or inter-pulse delay in two-pulse experiments are appropriately chosen to match the timescale of cluster expansion. Fig. 2 (after ref. 15 and 16) demonstrates the presence of an optimal two-pulse delay or pulse width for the occurrence of nanoplasma resonance with optical absorption and the highest observed ionic charge-state as experimental variables. In panel (a) the time-dependent absorption measured in a two-pulse study[15] evidences the optimal delay for maximal absorption, which increases with cluster size. In the case of Ag clusters,[16] a pulse width of 600 fs produced maximal charging across a range of peak intensities of the incident laser pulse. Saalmann *et al.*[20] established the occurrence of this resonance phenomenon by showing that the phase difference between motion of the center-of-mass of electrons in the nanoplasma and the driving laser pulse undergoes a π/2-flip at the same time as when the damping coefficient, which is a measure of laser pulse absorption, goes over a maximum.

Emission of ions, electrons and photons

Several studies spanning a wide-range of laser pulse and intensity parameters have reported the emission of highly-charged ions and energetic electrons resulting from the photoionization of clusters on sub-picosecond and picosecond timescales. In all such cases, the maximum observed charge-states for ions from the photoionization of clusters far exceeds that observed in isolated atoms – *e.g.*, Snyder *et al.*[21] observed a maximum charge-state of 20+ for Xe ions resulting from the irradiation of Xe clusters with 350 fs pulses with peak intensities of $\sim 10^{15}$ W cm^{-2}, whereas even with intensities as large as 10^{18} W cm^{-2}, the highest charge state observed for the case of isolated Xe atoms by Palaniyappan *et al.*[22] was only Xe^{12+} with nonsequential atomic photoionization processes reportedly becoming important. Also, in the case of metal clusters (Pb, Ag, Pt, Au), at peak intensities of 10^{16} W cm^{-2}, charge-states as high as 30+ have been observed consistently[23,24] in the long-pulse regime. The observation of higher charge-states in the case of cluster photoionization as compared to isolated atoms clearly indicates the important role of collective effects in the electron–ion dynamics in cluster nanoplasmas.

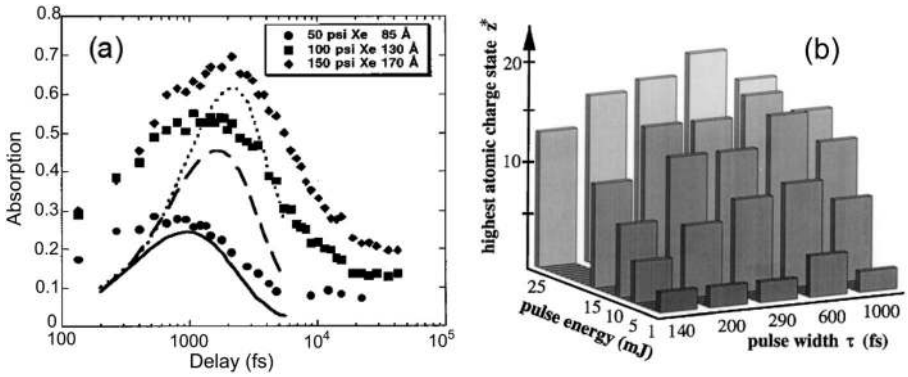

Fig. 2 Nanoplasma resonance – absorption and charging observed in experiments: (a) probe absorption as a function of delay between pump and probe pulses for different sizes of Xe clusters as reported in ref. 15 and (b) the maximum charge state measured by Köller *et al.*[16] resulting from the photoionization of pure Ag clusters as a function of pulse width for different pulse energies. Both (a) and (b) establish that nanoplasma resonance is a robust phenomenon underlying the ps and sub-ps dynamics. Copyright American Physical Society (1999), ref. 15 and 16.

Two key aspects of the dynamics leading to the charging of clusters are – (i) the high local fields in the electron ion system[8] and (ii) the gain in the kinetic energy of quasi-free electrons trapped in the potential of the ions.[7] The net potential of ions (U_{cluster}) in the cluster is largely harmonic[6] for relatively small displacements of the electron cloud from the center of charge of the ions:

$$U_{\text{cluster}}(r,R)=\left\{\begin{array}{c}-\frac{Q}{2R}\left(3-\frac{r^2}{R^2}\right), r\le R;\\ -\frac{Q}{r}, r\ge R\end{array}\right\}; \qquad (3)$$

where r is the radial coordinate, R is the cluster radius and Q is the net ionic charge in the cluster. For large excursions of the electron cloud, this net ionic potential has an anharmonic character.[25] The consequences of electron oscillations in both barrier-lowering for ionization as well as screening within the ionized cluster have been considered in detail by Fennel *et al.*[26] including a treatment of these effects in *ab initio* calculations. Furthermore, the local electric field in the cluster due to the relative displacement of the centers of charge of electrons and ions, respectively, also called the polarization field, dynamically changes as laser-driven dipolar oscillations of the electron cloud in the ionic cluster potential occur. This aids further charging of ions by lowering the effective Coulomb barrier and enhancing the rate of tunnel ionization in the cluster as compared to that of an isolated atom (see *e.g.* Krainov *et al.*[8]). An immediate consequence of this process is the following: the effect of the polarization field is anisotropic. The ions at the poles of the nanoplasma along the direction of laser polarization (and collective electron oscillation) are charged to a larger extent than those at the equator. Indeed, this was evidenced by Kumarappan *et al.*[27] who observed that photoions emanating parallel to the direction of laser polarization have kinetic energies larger than those released perpendicular to it. They attributed this to so-called ''charge-flipping'' which is essentially a consequence of the anisotropic polarization field as the simulations of Jungreuthmayer *et al.*,[28] shown in Fig. 3, revealed. We will see that this picture does not strictly hold in the case of few-cycle pulse photoionization.

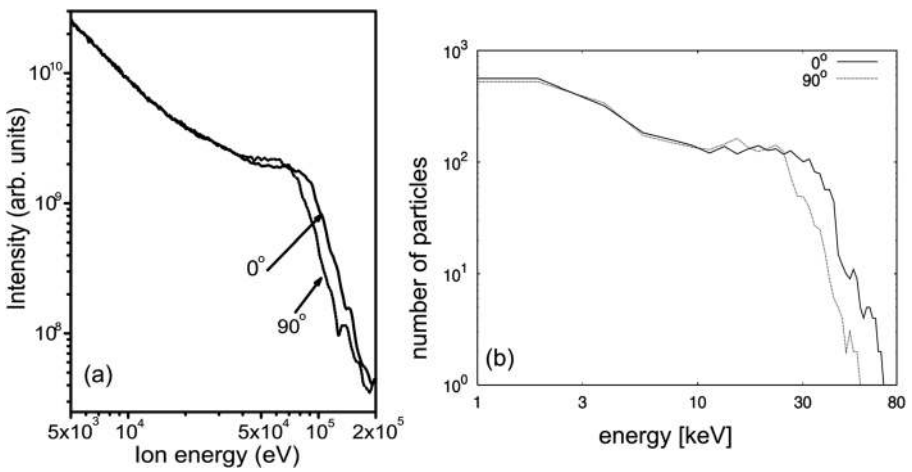

Fig. 3 Anisotropic ion emission: (a) experimentally measured ion kinetic energy spectra for $Ar_{40\,000}$ clusters exposed to 150 fs pulses with a peak intensity of 8×10^{15} W cm^{-2} in ref. 27 and (b) result of particle-in-cell simulations by Jungreuthmayer *et al.* as reported in ref. 28 performed for single clusters using similar parameters as in (a). In both panels the curve labelled 0° (90°) is the kinetic energy spectrum of ions emitted parallel (perpendicular) to the direction of the laser polarization. Copyright American Physical Society (2001 and 2004), ref. 27 and 28

Secondly, quasi-free electrons in the cluster can expend a part of the kinetic energy gained from laser field and ionize the ions further by inelastic collisions (*i.e.*, impact-ionization). The kinetic energy gained by a free electron driven in the laser field of intensity I (W cm^{-2}) and central wavelength λ (μm) is of the order of the ponderomotive energy given (in electron-volts) as $U_P = 9.33 \times 10^{-14} \cdot I \cdot \lambda^2$. In clusters, quasi-free electrons can gain kinetic energies as high as $\sim 50U_P$ or more. Lotz cross sections σ_c (ref. 29) have been used successfully to estimate the electron-impact ionization even in these dense nanoplasmas:

$$\sigma_c = a_i f_i \frac{\ln(K_e/\Phi_{IP})}{K_e \cdot \Phi_{IP}}; \quad (4)$$

where K_e is the electron kinetic energy, Φ_{IP} is the ionization potential for the removal of the next electron from the valence shell containing f_i electrons and a_i is a constant depending on the atomic species. The role and treatment of electron recombination in diminishing ionic charge within the cluster is a developing subject. Peltz *et al.*[30] have pointed out that the main recombination channel to be considered in these dense nanoplasmas is three-body recombination (TBR) – the capture of an electron by an ion in the vicinity of a second electron. It should be noted here, following Krainov *et al.*[31] and Peltz *et al.*,[30] that many high-lying Rydberg states may not be available for recombination due to the local fields in the plasma. Thus, a cut-off in the maximum principal quantum number should necessarily be employed in estimations of recombination rates. Impact-ionization is also most efficient under the conditions of resonant energy transfer between the laser field and the driven electron–ion system. Köller *et al.*[16] observed that the highest charge-states of photoions appear at optimal pulse durations ($\sim$600 fs) which remain constant over a wide range of intensities, corresponding to the occurrence of a nanoplasma resonance.

As expected from the preceding discussion on photoion emission, photoelectrons too may be expected to carry signatures of the strong anisotropic local polarization fields operating in the nanoplasma. Owing to collective oscillations and resonance in the nanoplasma, photoelectrons emitted from clusters have kinetic energy distributions with tails extending to more than $50U_P$,[7,32] whereas in the case of isolated atoms classical theory sets a limit of about $10U_P$.[33] In the case of Xe clusters, the ratio of the fast electron yield parallel to the laser polarization ($Y_\parallel$) to that of the perpendicular component ($Y_\perp$) was measured to be about 3.5,[34] while another study on Ag clusters demonstrated a $Y_\parallel/Y_\perp$ ratio greater than 6.[32] It should be mentioned that a direct comparison of these ratios between different experiments is difficult since the $Y_\parallel/Y_\perp$ depends on the solid-angle of collection of photoelectrons which is not necessarily the same in all studies. In the study on Ag clusters,[32] a comparison of experiments to *ab initio* calculations revealed a dominant mechanism for electron acceleration: quasi-free electrons which maintain an appropriate phase relationship with the plasmon oscillations synchronized with the laser field benefit from timely recollisions with the ionic core after excursions away from the center. This acceleration which occurs predominantly in the surface region of the ionic core due to the local polarization field in the nanoplasma has been appropriately termed as surface plasmon-assisted recollision (SPARC). Since the polarization field is maximal when nanoplasma resonance is achieved, the $Y_\parallel/Y_+$ ratio follows this trend.[32] Extending the phenomenon first observed in atoms, Saalmann *et al.*[35] provided an elegant generalization of the momentum gained by electrons following their recollision with an extended potential well. In the latter case, the momentum gain depends not only on the vector potential of the driving laser field but also on the length of the attractive potential in extended systems such as clusters.

An important consequence of the presence of highly-charged ions and energetic electrons is photo-emission from bound–bound transitions and recombination in these nanoplasmas, particularly in the inner atomic shells. Characteristic X-ray emission (*e.g.* K_α-X-rays) from a variety of clusters has been measured.[36–39] In the long-pulse regime, once again, short wavelength emission from inner-shell transitions was found to maximize at the optimal pulse-length (or -delay) corroborating nanoplasma resonance. Indeed, doping Ar clusters with ($\sim$1%) H_2O[37] led to an enhancement of the yield in Ar characteristic X-rays over pure Ar clusters. A similar enhancement in the maximal charge-state of Ar ions from HI doped Ar clusters has also been observed.[40]

In the long-pulse limit, cluster disintegration on ps time-scales has also led to several interesting consequences and has been used as a probe for effects of the dynamics during the interaction with the laser pulse. The expansion of the ionic core of the cluster, which is crucial for attaining nanoplasma resonance, also leads to a lowering of the height of the cluster potential that withholds quasi-free electrons from leaving the cluster. When this is no longer the case, electrons boil-off the cluster potential leaving behind a net positive charge. Both the pressure on ions due to mutual Coulombic repulsion as well as the (attractive) pressure of the expanding electron gas on ions act to dismantle the ionic core leading to high-energy photoion emission.[6,7] The resultant high kinetic energy of ions was exploited to demonstrate nuclear fusion in deuterium clusters.[41] Islam *et al.*[42] showed that the characteristic shape of ion kinetic energy spectra (Fig. 3) can be deduced by a combination of the Coulomb explosion profile of uniformly charged clusters with averaging over laser intensities in the focal volume, the distribution of cluster sizes and including possible saturation in the charging process. Subsequently, Peano *et al.*[43] showed that (at intensities $\sim 10^{16}$ W cm^{-2}) the shape of the ion kinetic energy distributions depends on the ratio of the Coulombic potential energy and the thermal energy of the electron gas, thus calling for a more careful application of the purely Coulombic picture. In cases where the cluster is stripped of most electrons at an early stage, ion kinetic energy distributions can carry signatures of phenomena such as formation of shock shells,[44] ion overtake[45] and indeed even alignment in molecular clusters.[46] As a result, deriving information about the dynamics ensuing during the interaction with the laser pulses from such ion kinetic energy distributions (without resolving their charge-states) is not straightforward. A recent development

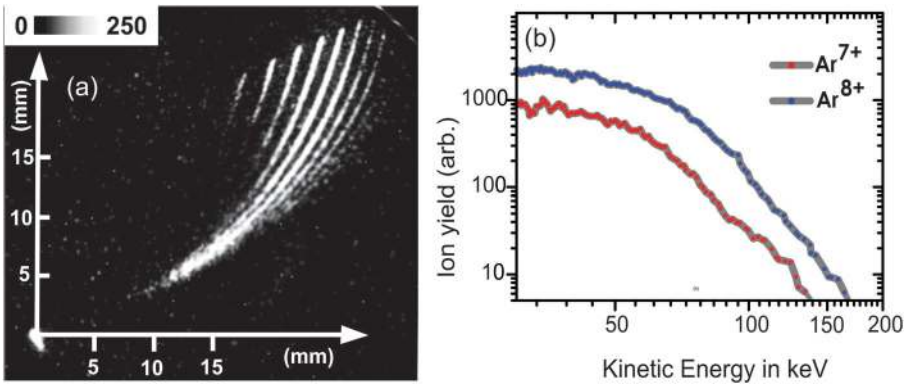

Fig. 4 Benchmark two-dimensional charge-state resolved ion kinetic energy distributions: using a Thomson parabola spectrometer (see ref. 47 for details) kinetic energy distributions of the different charge-states of ions resulting from the photoionization of Ar clusters by 150 fs pulses ($\sim 10^{16}$ W cm^{-2}) can be obtained. (a) The ''parabolas'' seen as is on the imaging microchannel plate detector are shown. Along each parabola, the mass/charge of the impinging ion remains constant while the kinetic energy varies. The charge-states increase from left to right and the three representative charge-states of positively charged Ar ions, 3, 5 and 7 are marked. (b) The kinetic energy distributions of Ar^{7+} and Ar^{8+} ions obtained from the corresponding parabolas in (a) are presented, for details of the procedure see ref. 47.

in this regard is the demonstration of obtaining two-dimensional kinetic energy distributions of ions by the group led by one of the authors[47,48] – the kinetic energy distributions of each individual ionic charge-state can be obtained using Thomson parabola spectrometers. A benchmark two-dimensional spectrum and the kinetic energy distributions are presented in Fig. 4. The use of this spectrometer in combination with time-of-flight analysis led to the discovery that high-energy neutral atoms as well as fast negative ions from molecular clusters can be generated using cluster nanoplasmas.[48]

Intense near-IR few-cycle pulses and photoionization of clusters

It is clear from the preceding discussions that cluster expansion and ionic motion are necessary for nanoplasma resonance to occur on ps and sub-ps timescales. This mechanism is essentially turned-off by employing few-cycle pulses ($\sim$10 fs) since the motion of ions can be neglected on these timescales.[6,7] Consequently, few-cycle pulses act as an ''impulse'' with regard to ionic motion. By excluding the key operational mechanism in the long-pulse case, few-cycle pulses open up a new regime for exploration. The remainder of this article is devoted to the new science emerging on these timescales.

Generation and use of intense few-cycle pulses

Amplified few-cycle pulses at NIR wavelengths with durations as short as 10 fs are produced using mode-locked Ti:Sapphire based laser systems. Following conventional chirped-pulse amplification, spectral broadening using a gas-filled hollow fiber and subsequent recompression by chirped-dielectric mirrors produce few-cycle pulses with typical energies as high as a few mJ at repetition rates higher than 1 kHz.[1] The width of these pulses is measured using well-established techniques such as coherent autocorrelation, frequency-resolved optical gating and spectral interferometry.[49] Typically, these pulses are focussed onto a cluster jet in a vacuum chamber and photo-fragments are subsequently measured using a suitable spectrometer.[54]

Photoion emission – a counter-intuitive picture

We measured the photoion kinetic energy spectrum from Ar clusters subject to 7 fs pulses with an intensity of 2×10^{15} W cm^{-2} which is presented in Fig. 5. Clearly, the ion kinetic energy (KE) distribution is very similar to observations in the long-pulse regime (Fig. 3). Although the physics of ion emission in this ''frozen'' regime seems similar to the long-pulse case, a comparison of ion KE distributions parallel and perpendicular, relative to the laser polarization direction, reveals a surprising counter-intuitive phenomenon. Unlike in the long-pulse case, the maximum KE of ions in the direction perpendicular to the laser polarization ($E_\perp$) is greater than that of the ions emerging in the parallel ($E_\parallel$) direction, $E_\perp > E_\parallel$, as reported by Skopalová *et al.*[50] and is evident in Fig. 6. Similar observations were also

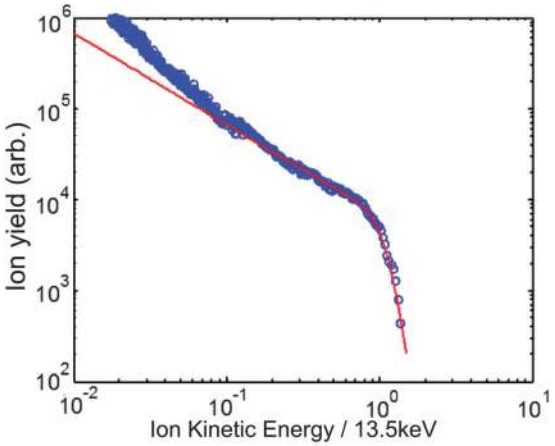

Fig. 5 Ion kinetic energy distribution from Ar clusters photoionized by 7 fs pulses with a peak intensity of 2×10^{15} W cm^{-2}. The data (blue circles) are best-fit (red line) with the scheme of Islam *et al.*[42]

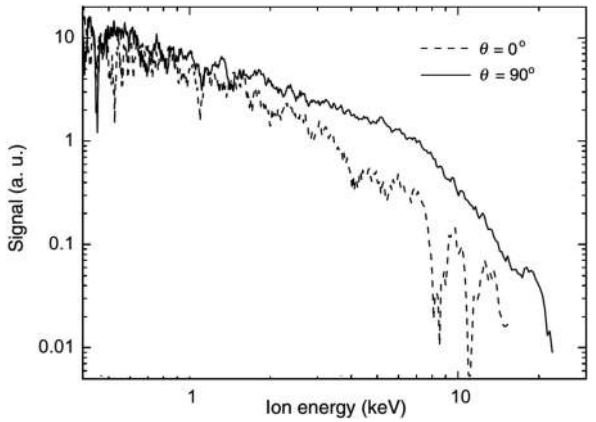

Fig. 6 Anomalous anisotropy in the kinetic energy distribution of ions in the few-cycle regime as reported by Skopalová *et al.*[50] The ions emerging parallel to the direction of laser polarization (0°, dotted curve) and those emanating perpendicular to it (90°, solid curve) are shown. This picture is in contrast to the observation made in the long-pulse regime presented (see Fig. 3), as discussed in the text. Copyright American Physical Society (2010), ref. 50.

made independently following this study.[51,52] The picture of a strong polarization force within the cluster leading to higher charging at the poles in the long-pulse regime[27] leading to $E_{\parallel} > E_{\perp}$ does not hold in the case of few-cycle pulses. Indeed, Skopalová *et al.*[50] recovered the latter case ($E_{\parallel} > E_{\perp}$) by stretching the pulses to durations longer than 150 fs, when ionic motion in these systems sets in. They reasoned the counter-intuitive behaviour in the impulse regime ($E_{\perp} > E_{\parallel}$) using the motion of a uniform quasi-free electron cloud with a size smaller than the cluster ionic core. As a consequence of their limited extent within the cluster, the electron cloud repeatedly screens the poles during the driven oscillations but leaves the equatorial region unscreened. Thus, greater charge develops along the equator leading to the observed anomalous anisotropy.[50,53] Although a qualitative picture has emerged to account for the atypical anisotropy observed in the impulsive regime, the role of screening and recombination, which is well-understood in the long-pulse regime,[30,54] needs to be investigated in detail for the case of few-cycle pulses. Sub-cycle dynamics leading to breaking of the plasma waves in the cluster and the consequent formation of "hot-spots" on few-femtosecond timescales examined by Varin *et al.*[55] could also play a significant role in the interaction with such short pulses.

Designing nanoplasmas for resonances in few-cycle pulses and dopant-induced ignition

It is clear from the discussions in the preceding sections dedicated to the long-pulse limit that ionic motion on sub-ps timescales is a necessary pre-requisite to bring the over-dense cluster nanoplasma to sufficient dilution whereby a resonance between the collective electron oscillations and the driving laser field can occur. Thus, on timescales of 10 fs or less, when the ionic core remains frozen, conventional nanoplasma resonance due to cluster expansion cannot occur. Mikaberidze *et al.*[56] pointed out a mechanism for the resonant coupling of laser pulses which can occur due to nanoplasma morphology, without the need for ionic motion or the consequent lowering of plasma density within the cluster. They proposed ionizing a doped He nanodroplet (with the dopant Xe atoms residing at the center) using laser pulses which have a carefully chosen intensity such that only the dopants, but not the He atoms, are directly ionized by the optical field. Beginning with the "seed" electrons released from the Xe atoms, the ionization of He occurs as the linearly polarized laser field drives them along the direction of its oscillating electric field. Consequently, the ionization of the doped droplet proceeds inside-out and a nanoplasma is created inside the neutral host medium as the laser pulse ramps in intensity. Remarkably, the resonant coupling of the laser field with this ellipsoidal nanoplasma leads to the complete ionization of all the 10^4 host atoms in the He nanodroplet even with a very weak doping of less than 10 Xe atoms. The experiments by Krishnan *et al.*[57] confirm this: under intense 10 fs pulse irradiation, the yield of He^+ and He^{2+} ions as a function of the number of doped Xe atoms in the He nanodroplets (containing 15 000 He atoms on average) was found to increase sharply and saturate for a doping number of just 7 leading to dopant-induced ignition, as shown in Fig. 7.

The main reason underlying this dramatic turnaround from transparent pure He nanodroplets to active doped clusters is the onset of a new nanoplasma resonance mechanism occurring on timescales less than 10 fs. Similar to the long-pulse case, understanding the interaction between few-cycle pulses and these doped droplets requires an examination of the interrelation between the laser frequency (ω) and the eigenfrequencies of the embedded nanoplasma. Since this nanoplasma is formed by the collective driving of electrons along the direction of laser polarization, the morphology of the electron–ion system is ellipsoidal, or cigar-shaped.[56] The ellipsoidal ionic potential in which the quasi-free electrons oscillate has two characteristic frequencies – the first is the eigenfrequency for oscillations along

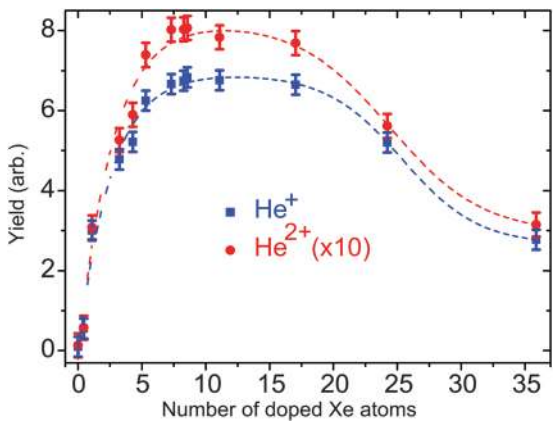

Fig. 7 Dopant-induced ignition: the yield of He^+ and He^{2+} ions from Xe doped He nanodroplets as a function of the number of doped atoms, after ref. 57. The charging of the nanoplasma in droplets containing 10^4 He atoms saturates for a doping number of just 7. The fall in yield at large doping numbers (>20 doped Xe atoms) is due to the destruction of the droplet beam. Copyright American Physical Society (2011), ref. 57.

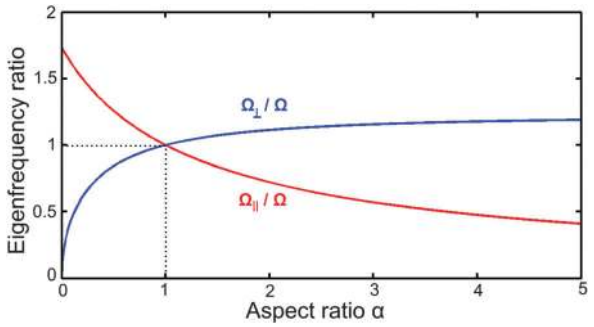

Fig. 8 Eigenfrequencies of the ellipsoidal nanoplasma along the major and minor axes as a function of the ellipsoid aspect ratio (α), scaled by the eigenfrequency for a spherical plasma with identical charge density [see also ref. 56, 58 and 59].

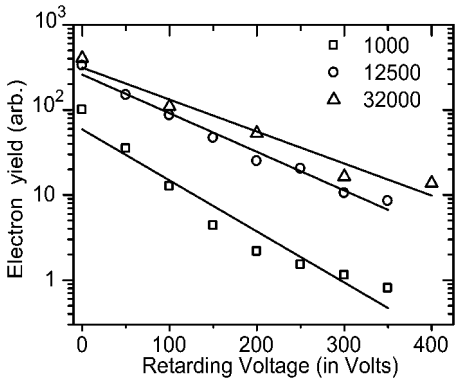

Fig. 9 Retarding potential analysis of photoelectrons emitted by Ar clusters of different sizes (in the legend) ionized by 7 fs pulses ($\sim 10^{15}$ W cm^{-2}): the temperatures of the distributions are 46 eV, 81 eV and 107 eV for clusters containing 1000 (□), 12 500 (○) and 32 000 (△) Ar atoms per cluster, respectively. Lines to guide the eye.

the major axis of the ellipse parallel to the laser polarization vector $\Omega_{\parallel}$, while the other mode orthogonal to the driving electric field has a natural frequency $\Omega_{\perp}$. These eigenfrequencies depend on the charge density ρ and the aspect ratio α of the ellipsoid. Using the eigenfrequency (Ω) of a spherical nanoplasma with an identical charge density ρ, (see eqn (1)), $\Omega_{\parallel}$ and $\Omega_{\perp}$ may be written as:[58,59]

$$\Omega_{\parallel} = \Omega \cdot g(\alpha) \text{ and } \Omega_{\perp} = \Omega \cdot h(\alpha); \quad (5)$$

where, $g(\alpha)$ and $h(\alpha)$ are decreasing and increasing functions of α, respectively. The detailed expressions for $g(\alpha)$ and $h(\alpha)$ plotted in Fig. 8 can be found in ref. 58 and 59. Since the aspect ratio of the nanoplasma increases with the growth of charge within the nanodroplet, the relevant eigenfrequency component $\Omega_{\parallel}$ drops and matches the driving frequency of the laser (ω): $\Omega_{\parallel} = \omega$.

Fortuitously, this condition is achieved close to the intensity peak of the pulse,[56] whereupon resonant driving of electrons leads to the complete ionization of the host He atoms.

Photoelectron emission

The emission of photoelectrons from cluster nanoplasmas in intense few-cycle pulse interactions is an aspect of the dynamics complimentary to photoion generation. El-Taha *et al.*[60] measured photoelectron emission from Xe clusters with a time-delayed pair of $\sim$11 fs pulses and intensity fractions of 0.3 and 0.7 for the first (leading) and second (probe) pulses respectively. The measured electron yields showed a characteristic pump–probe dependence on a ps-timescale. The maximum yield of electrons was found to occur at an optimal delay which depended on the size of the cluster. It should be mentioned that although this two-pulse study employs few-cycle pulses, the phenomenology investigated clearly belongs to the long-pulse regime.

We present here for the first-time, to the best of our knowledge, photoelectron emission measurements in the few-cycle limit. Our experimental set-up is similar to those employed in several previous investigations.[61] In our experiment, Ar clusters (sizes in the range 1000–32 000) were ionized by 7 fs pulses ($\sim 10^{15}$ W cm^{-2}). The time-of-flight spectra of photoelectrons were recorded using a microchannel plate detector. In order to obtain signals specific to photoelectrons and differentiate these from photons which could simultaneously arrive at the detector due to delayed photoemissions, we employed a retarding electric field ahead of the detector which allowed us to selectively collect only those photoelectrons which have a kinetic energy sufficient to overcome this applied potential barrier. Indeed applying retarding potentials is important as the studies of Springate *et al.*[62] and Kumarappan *et al.*[34] revealed.

Fig. 9 shows the relative electron yield as a function of the retarding voltage applied for 3 different sizes of Ar clusters – 1000, 12 500 and 32 000 atoms per cluster. From these integrated electron yields as a function of retarding voltage, we obtain the photoelectron temperatures following the method used by Jha *et al.*[61] Noting that the photoelectrons emitted have an exponential distribution of kinetic energies, we may write the corresponding energy distribution function as:

$$s(E) = s_0 \exp(-E/k_B T); \quad (6)$$

where k_B is the Boltzmann constant, T is the temperature of the distribution, E is the photoelectron kinetic energy and s_0 is a constant. Since the application of a retarding potential V results in the detector collecting photoelectrons with kinetic energies $E > V$, the yield of electrons measured by the detector as a function of the retarding potential $S(V)$ is:

$$S(V) = \int_{E>V}^{\infty} dE s_0 \cdot \exp(-E/k_B T) = s_0^2 kT \cdot \exp(-V/k_B T); \quad (7)$$

It is clear from eqn (7) that the temperature of the photoelectron kinetic energy distribution can be obtained from $S(V)$. Employing this method which was also used by Jha *et al.*,[61] we determined that the temperature of the photoelectrons from these Ar nanoplasmas increases from 46 eV to 107 eV as the size of the cluster is increased from 1000 to 32 000 atoms per aggregate. The temperatures measured here are in the range of values obtained earlier[61] with 150 fs pulses ($\sim 10^{15}$ W cm^{-2}) in the nonimpulsive regime. However, it is clear from the work of Skopalová *et al.*[50] on Ar (and Xe) clusters that the key aspects such as the extent of the electron cloud within the cluster are

fundamentally different in the impulsive regime as compared to the long-pulse case. Thus, acceleration mechanisms from which electrons gain their kinetic energy are significantly different in the few-cycle limit. The work of Varin *et al.*[55] provides valuable insights into the role and importance of sub-cycle phenomena occurring on attosecond timescales relevant in this context – the coupling of intense laser pulses to confined media in only a few optical cycles involves the formation and eventual breaking of plasma waves. But clearly, further theoretical and experimental investigations are required to uncover the rich underlying physics and our studies motivate the same.

Carrier envelope phase effects

For pulses with a central wavelength of 800 nm, the carrier wave has an optical cycle less than 3 fs. As a result, in pulses with a temporal full-width at half-maximum of 5 fs or less, the shape of the electric field within the temporal envelope of the pulse becomes an important factor. This unique feature of few-cycle pulses can be quantified by the relative phase between the maxima of the pulse envelope and that of the electric field of the carrier wave within. This phase can be measured experimentally and is called the carrier-envelope phase (CEP), denoted by φ_{CE} in Fig. 10(a).[63] Formally, the time-dependent electric field $E(t)$ can be written in terms of the envelope function $E_0(t)$, the angular frequency of the carrier wave ω and the CEP represented by φ_{CE} as, $E(t) = E_0(t)\cdot\cos(\omega t + \varphi_{CE})$. Single-shot CEP measurements have been demonstrated and used to perform experiments on atomic systems.[63] In the case of atoms and molecules, several studies have demonstrated that electron dynamics depends upon the CEP of the pulse and can even be controlled using the same (see *e.g.*, ref. 2–5).

Currently, there are but a few studies on CEP effects in the photoionization of nanoscale media. Zherebtsov *et al.*[64,65] reported impressive studies on the photoionization of silica (SiO_2) nanoparticles with diameters of 50–150 nm using 5 fs pulses having intensities in the range 1–5 $\times$ 10^{13} W cm^{-2}. They measured and compared the kinetic energies of photoelectrons emitted from Xe atoms and silica nanospheres along the direction of polarization of the electric field of the incident laser pulse. In the case of phenomena that depend on the time varying electric-field of an incident laser pulse such as photoelectron emission, the CEP of the linearly polarized few-cycle pulse breaks the inversion symmetry of experimental observables along the polarization axis leading to a "stereo" effect.[63] In order to quantify this, we use labels "up" and "down" to designate the two directions with an angular separation of π along the polarization axis as shown in Fig. 10(a). The asymmetry of photoelectron emission between the up- and down-directions gives a quantitative measure of the associated CEP sensitivity:[63] If Y_{UP} and Y_{DOWN} are, respectively, the yields of photoelectrons with a given kinetic energy or momentum emitted into the "up" and "down" hemispheres from the photoexcitation by a vertically polarized few-cycle pulse, the CEP-dependent asymmetry parameter can be defined as $A(\varphi_{CE}) = (Y_{UP} - Y_{DOWN})/(Y_{UP} + Y_{DOWN})$. Fig. 10(b) clearly shows the dependence of the asymmetry parameter as a function of both CEP and photoelectron momentum along the axis of linear polarization of the incident few-cycle pulse, measured by Zherebtsov *et al.*[65] The peak intensity of the pulses used in this case was 3.7 $\times$ 10^{13} W cm^{-2}, corresponding to a ponderomotive energy of U_P of $\sim$1.5 eV. In contrast to the photoelectrons from Xe atoms which carried away a maximum kinetic energy of about $10U_P$, the observed cut-off in the nanoparticle case extended beyond $50U_P$, clearly evidencing the collective phenomena in clusters. An immediate conclusion from the observed CEP dependence is that the electron acceleration mechanisms dominant in extended systems depend on the instantaneous electric field of the laser and sub-cycle phenomena therein are important. This also paves way to the control and manipulate these processes by manoeuvring the shape of the electric field within the pulse.

Furthermore, a report by Köhn and Fennel in this journal[66] suggested spectral interferometry as a means of extracting information about the dynamics occurring in sub-cycle timescales based on a theoretical microscopic analysis: characteristics

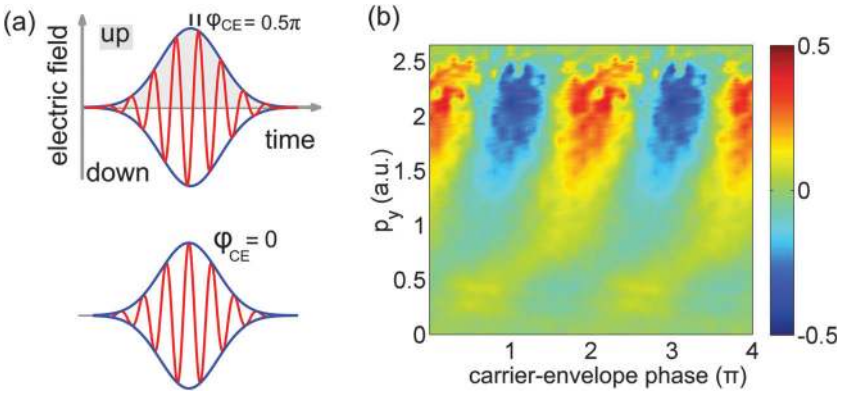

Fig. 10 (a) The carrier-envelope phase (CEP) of a few-cycle optical pulse: CEP is the phase offset between the maximum of the envelope of the pulse (blue) and the maximum of the electric field (red) within the envelope. Two cases where the CEP has values 0.5π and zero, respectively, are shown. (b) The asymmetry parameter (defined in the text) as a function of the carrier envelope phase (horizontal axis) and the electron momentum (labelled p_y, in atomic units, vertical axis) along the direction of polarization of the laser electric field, reported by Zherebtsov *et al.* in ref. 65. Reproduced with permission – copyright Institute of Physics.

of collective electron motion, namely the period and lifetime of plasmon oscillations along with the phase and relative amplitude can possibly be extracted with sub-femtosecond resolution, while the experimental realization of this scheme remains to be seen. Similarly, Kundu *et al.*[25,67] suggested using harmonic emission from clusters as a probe for possible nonlinear resonances occurring in the collective electron motion in clusters within a few optical cycles due to the anharmonicity of the ionic potential in pristine clusters. Successful observation of these optical emissions requires significantly large number densities of clusters ($>10^8$ per cm^3) as can be obtained near the exit of nozzles used for producing these aggregates as well as developing schemes to distinguish these coherent emissions from that due to recombination or atomic transitions.

Conclusions and outlook

Intense few-cycle near-IR pulses have opened up a plethora of intriguing phenomena and physics to be investigated in the near future. In comparison with the long-pulse regime, counter-intuitive observations like the anomalous anisotropy in ion emission as well as the need to understand effects carried over from the long-pulse case into the impulse regime such as the acceleration of electrons to kinetic energies of the order of $\sim$500 eV within 10 fs require a combination of experiments and theory to lead to better insights. A natural extension of these studies with few-femtosecond pulses is the use of isolated as well as trains of attosecond pulses as probes for the collective dynamics. Indeed, photoemission in solids investigated using attosecond pulses[68] and observation of phenomena such as metallization of insulators[69] on sub-fs timescales are areas open for research. Finally, using few-cycle IR pulses in combination with extreme-ultraviolet pulses from table-top sources as well as soft- and hard-Xray pulses from free-electron lasers[70] are exciting prospects for the future and are forthcoming perspectives.

Notes and references

1 T. Brabec and F. Krausz, *Rev. Mod. Phys.*, 2000, **72**, 545.
2 R. Gopal, K. Simeonidis, R. Moshammer, Th. Ergler, M. Dürr, M. Kurka, K.-U. Kühnel, S. Tschuch, C.-D. Schröter, D. Bauer and J. Ullrich, *Phys. Rev. Lett.*, 2009, **103**, 053001.
3 M. F. Kling, Ch. Siedschlag, A. J. Verhoef, J. I. Khan, M. Schultze, Th. Uphues, Y. Ni, M. Uiberacker, M. Drescher, F. Krausz and M. J. J. Vrakking, *Science*, 2006, **312**, 246.
4 M. Kremer, B. Fischer, B. Feuerstein, V. L. B. de Jesus, V. Sharma, C. Hofrichter, A. Rudenko, U. Thumm, C. D. Schröter, R. Moshammer and J. Ullrich, *Phys. Rev. Lett.*, 2009, **103**, 213003.
5 B. Fischer, M. Kremer, T. Pfeifer, B. Feuerstein, V. Sharma, U. Thumm, C. D. Schröter, R. Moshammer and J. Ullrich, *Phys. Rev. Lett.*, 2010, **105**, 223001.
6 U. Saalmann, Ch. Siedschlag and J.-M. Rost, *J. Phys. B: At., Mol. Opt. Phys.*, 2006, **39**, R39.
7 Th. Fennel, K.-H. Meiwes-Broer, J. Tiggesbäumker, P.-G. Reinhard, P. M. Dinh and E. Suraud, *Rev. Mod. Phys.*, 2010, **82**, 1793.
8 V. Krainov and M. B. Smirnov, *Phys. Rep.*, 2002, **370**, 137.
9 M. Protopapas, C. H. Keitel and P. L. Knight, *Rep. Prog. Phys.*, 1997, **60**, 389.
10 O. F. Hagena and W. Obert, *J. Chem. Phys.*, 1972, **56**, 1793.
11 R. A. Smith, T. Ditmire and J. W. G. Tisch, *Rev. Sci. Instrum.*, 1998, **69**, 3798.
12 F. Dorchies, F. Blasco, T. Caillaud, J. Stevefelt, C. Stenz, A. S. Boldarev and V. A. Gasilov, *Phys. Rev. A*, 2003, **68**, 023201.
13 F. Stienkemeier and K. Lehmann, *J. Phys. B: At., Mol. Opt. Phys.*, 2006, **39**, R127.
14 J. P. Toennies and A. F. Vilesov, *Angew. Chem.*, 2004, **43**, 2622.
15 J. Zweiback, T. Ditmire and M. D. Perry, *Phys. Rev. A*, 1999, **59**, 3166.
16 L. Köller, M. Schumacher, J. Köhn, S. Teuber, J. Tiggesbäumker and K. H. Meiwes-Broer, *Phys. Rev. Lett.*, 1999, **82**, 3783–3786.
17 U. Even, J. Jortner, D. Noy, N. Lavie and C. Cossart-Magos, *J. Chem. Phys.*, 2000, **112**, 8068.
18 J. Tiggesbäumker and F. Stienkemeier, *Phys. Chem. Chem. Phys.*, 2007, **9**, 4748.
19 O. Bünermann and F. Stienkemeier, *Eur. Phys. J. D*, 2011, **61**, 645.
20 U. Saalmann and J.-M. Rost, *Phys. Rev. Lett.*, 2003, **91**, 223401.
21 E. M. Snyder, S. A. Buzza and A. W. Castleman Jr, *Phys. Rev. Lett.*, 1996, **77**, 3347.
22 S. Palaniyappan, A. DiChiara, I. Ghebregziabher, E. L. Huskins, A. Falkowski, D. Pajerowski and B. C. Walker, *J. Phys. B: At., Mol. Opt. Phys.*, 2006, **39**, S357.
23 M. A. Lebeault, J. Viallon, J. Chevaleyre, C. Ellert, D. Normand, M. Schmidt, O. Sublemontier, C. Guet and B. Huber, *Eur. Phys. J. D*, 2002, **20**(2), 233–242.
24 M. Schumacher, S. Teuber, L. Köller, J. Köhn, J. Tiggesbäumker and K. H. Meiwes-Broer, *Eur. Phys. J. D*, 1999, **9**, 411.
25 M. Kundu and D. Bauer, *Phys. Rev. Lett.*, 2006, **96**, 123401.
26 Th. Fennel, L. Ramunno and T. Brabec, *Phys. Rev. Lett.*, 2007, **99**, 233401.
27 V. Kumarappan, M. Krishnamurthy and D. Mathur, *Phys. Rev. Lett.*, 2001, **87**, 085005.
28 C. Jungreuthmayer, M. Geissler, J. Zanghellini and T. Brabec, *Phys. Rev. Lett.*, 2004, **92**, 133401.
29 W. Lotz, *Z. Phys.*, 1968, **241**, 216.
30 Ch. Peltz and T. Fennel, *Eur. Phys. J. D*, 2011, **63**, 281.
31 V. P. Krainov and A. V. Sofronov, *Contrib. Plasma Phys.*, 2007, **47**, 234.
32 T. Fennel, T. Döppner, J. Passig, C. Schaal, J. Tiggesbäumker and K. H. Meiwes-Broer, *Phys. Rev. Lett.*, 2007, **98**, 143401.
33 G. G. Paulus, W. Becker, W. Nicklich and H. Walther, *J. Phys. B: At., Mol. Opt. Phys.*, 1994, **27**, L703.
34 V. Kumarappan, M. Krishnamurthy and D. Mathur, *Phys. Rev. A*, 2003, **67**, 043204.

35 U. Saalmann and J.-M. Rost, *Phys. Rev. Lett.*, 2008, **100**, 133006.
36 V. Kumarappan, M. Krishnamurthy, D. Mathur and L. C. Tribedi, *Phys. Rev. A*, 2001, **63**, 023203.
37 J. Jha, D. Mathur and M. Krishnamurthy, *J. Phys. B: At., Mol. Opt. Phys.*, 2005, **38**, L291.
38 C. Deiss, N. Rohringer, J. Burgdörfer, E. Lamour, C. Prigent, J.-P. Rozet and D. Vernhet, *Phys. Rev. Lett.*, 2006, **96**, 013203.
39 J. Jha and M. Krishnamurthy, *Appl. Phys. Lett.*, 2008, **92**, 191108.
40 J. Purnell, E. M. Snyder, S. Wei and A. W. Castleman Jr., *Chem. Phys. Lett.*, 1994, **229**, 333.
41 T. Ditmire, J. Zweiback, V. P. Yanovsky, T. E. Cowan, G. Hays and K. B. Wharton, *Nature*, 1999, **398**, 489.
42 Md. R. Islam, U. Saalmann and J. M. Rost, *Phys. Rev. A*, 2006, **73**, 041201(R).
43 F. Peano, F. Peinetti, R. Mulas, G. Coppa and L. O. Silva, *Phys. Rev. Lett.*, 2006, **96**, 175002.
44 M. Grech, R. Nuter, A. Mikaberidze, P. Di Cintio, L. Gremillet, E. Lefebvre, U. Saalmann, J. M. Rost and S. Skupin, *Phys. Rev. E: Stat., Nonlinear, Soft Matter Phys.*, 2011, **84**, 056404.
45 M. Hohenberger, D. R. Symes, K. W. Madison, A. Sumeruk, G. Dyer, A. Edens, W. Grigsby, G. Hays, M. Teichmann and T. Ditmire, *Phys. Rev. Lett.*, 2005, **95**, 195003.
46 U. Saalmann, A. Mikaberidze and J.-M. Rost, *Phys. Rev. Lett.*, 2013, **110**, 133401.
47 R. Rajeev, K. P. M. Rishad, T. Madhu Trivikram, V. Narayanan and M. Krishnamurthy, *Rev. Sci. Instrum.*, 2011, **82**, 083303.
48 R. Rajeev, T. Madhu Trivikram, K. P. M. Rishad, V. Narayanan, E. Krishnakumar and M. Krishnamurthy, *Nat. Phys.*, 2013, **9**, 185.
49 *Few-Cycle Laser Pulse Generation and Its Applications*, ed. F. X. Kärtner, Springer, 2004, vol. 95.
50 E. Skopalová, Y. C. El-Taha, A. Zaïr, M. Hohenberger, E. Springate, J. W. G. Tisch, R. A. Smith and J. P. Marangos, *Phys. Rev. Lett.*, 2010, **104**, 203401.
51 D. Mathur and F. A. Rajgara, *J. Chem. Phys.*, 2010, **133**, 061101.
52 D. Mathur, F. A. Rajgara, A. R. Holkundkar and N. K. Gupta, *Phys. Rev. A*, 2010, **82**, 025201.
53 G. Mishra and N. K. Gupta, *Europhys. Lett.*, 2011, **96**, 63001.
54 S. R. Krishnan, Ch. Peltz, L. Fechner, V. Sharma, M. Kremer, B. Fischer, N. Camus, T. Pfeifer, J. Jha, M. Krishnamurthy, C.-D. Schröter, J. Ullrich, F. Stienkemeier, R. Moshammer, Th. Fennel and M. Mudrich, *New J. Phys.*, 2012, **14**, 075016.
55 C. Varin, C. Peltz, T. Brabec and T. Fennel, *Phys. Rev. Lett.*, 2012, **108**, 175007.
56 A. Mikaberidze, U. Saalmann and J. M. Rost, *Phys. Rev. Lett.*, 2009, **102**, 128102.
57 S. R. Krishnan, L. Fechner, M. Kremer, V. Sharma, B. Fischer, N. Camus, J. Jha, M. Krishnamurthy, T. Pfeifer, R. Moshammer, J. Ullrich, F. Stienkemeier, M. Mudrich, A. Mikaberidze, U. Saalmann and J.-M. Rost, *Phys. Rev. Lett.*, 2011, **107**, 173402.
58 S. R. Krishnan, PhD thesis, University of Heidelberg, 2011; A. Mikaberidze, PhD thesis, Technical University, Dresden, 2012.
59 L. D. Landau and E. M. Lifschitz, *Course of theoretical physics: The classical theory of fields*, Pergamon Press, 2009, vol. 2.
60 Y. C. El-Taha, E. Springate, R. Carley, F. Rajgara, D. Darios, C. Froud, S. Bonora, D. Symes, J. W. G. Tisch, R. A. Smith, D. Mathur and J. P. Marangos, *Lasers and Electro-Optics*, 2008, ISBN 978-1-55752-859-9.
61 J. Jha and M. Krishnamurthy, *J. Phys. B: At., Mol. Opt. Phys.*, 2008, **41**, 041002.
62 E. Springate, S. A. Aseyev, S. Zamith and M. J. J. Vrakking, *Phys. Rev. A*, 2003, **68**, 053201.
63 T. Wittmann, B. Horvath, W. Helml, M. G. Schätzel, X. Gu, A. L. Cavalieri, G. G. Paulus and R. Kienberger, Absolute-phase phenomena in photoionization with few-cycle laser pulses, *Nature*, 2001, **414**, 182.
64 S. Zherebtsov, T. Fennel, J. Plenge, E. Antonsson, I. Znakovskaya, A. Wirth, O. Herrweth, F. Süßmann, Ch. Peltz, I. Ahmad, S. A. Trushin, V. Pervak, S. Karsch, M. J. J. Vrakking, B. Langer, C. Graf, M. I. Stockman, F. Krausz, E. Rühl and M. F. Kling, *Nat. Phys.*, 2011, **7**, 656.
65 S. Zherebtsov, F. Süßmann, C. Peltz, J. Plenge, K. J. Betsch, I. Znakovskaya, A. S. Alnaser, N. G. Johnson, M. Kübel, A. Horn, V. Mondes, C. Graf, S. A. Trushin, A. Azzeer, M. J. J. Vrakking, G. G. Paulus, F. Krausz, E. Rühl, T. Fennel and M. F. Kling, *New J. Phys.*, 2012, **14**, 075010.
66 J. Köhn and T. Fennel, *Phys. Chem. Chem. Phys.*, 2011, **13**, 8747.
67 M. Kundu, S. V. Popruzhenko and D. Bauer, *Phys. Rev. A*, 2007, **76**, 033201.
68 M. Schultze, *et al.*, *Science*, 2010, **328**, 1658.
69 M. Durach, A. Rusina, M. F. Kling and M. I. Stockman, *Phys. Rev. Lett.*, 2010, **105**, 086803.
70 J. Ullrich, A. Rudenko and R. Moshammer, *Annu. Rev. Phys. Chem.*, 2012, **63**, 635.

